OPEN

1D Magnetic Materials of Fe_3O_4 and Fe with High Performance of Microwave Absorption Fabricated by Electrospinning Method

Rui Han[1], Wei Li[1], Weiwei Pan[2], Minggang Zhu[1], Dong Zhou[1] & Fa-shen Li[2]

[1]Functional Materials Research Institute, Central Iron and Steel Research Institute, Beijing 100081, P.R.China and Beijing Key Laboratory of Precision Alloys, Beijing 100081, China, [2]Institute of Applied Magnetics, Key Laboratory of Magnetism and Magnetic Materials of the Ministry of Education, Lanzhou University, Lanzhou 730000, P. R. China.

Fe_3O_4 and Fe nanowires are successfully fabricated by electrospinning method and reduction process. Wiry microstructures were achieved with the phase transformation from α-Fe_2O_3 to Fe_3O_4 and Fe by partial and full reduction, while still preserving the wire morphology. The diameters of the Fe_3O_4 and Fe nanowires are approximately 50–60 nm and 30–40 nm, respectively. The investigation of microwave absorption reveals that the Fe_3O_4 nanowires exhibit excellent microwave absorbing properties. For paraffin-based composite containing 50% weight concentration of Fe_3O_4 nanowires, the minimum reflection loss reaches -17.2 dB at 6.2 GHz with the matching thickness of 5.5 mm. Furthermore, the calculation shows that the modulus of the ratio between the complex permittivity and permeability $|\varepsilon/\mu|$ is far away from unity at the minimum reflection loss point, which is quite different from the traditional opinions.

One-dimensional (1D) nanomaterials such as nanotubes, nanowires, nanofibers and nanobelts have drawn considerable attention over the past few decades. These artificial nanomaterials allow one to explore novel physical properties that are distinct from those of their counterparts in nature. In particular, 1D magnetic nanomaterials are of considerable interest due to the fact that the geometrical dimensions of these materials become comparable to key magnetic length scales, such as the exchange length or the domain wall width[1–5]. On the other hand, the magnetic nanowires are also scientifically interesting because they can be considered as model systems to study interaction processes and magnetic reversal in low-dimensional magnetic structures[6,7]. Therefore, the synthesis of 1D magnetic nanostructure has attracted tremendous attention. Hematite (α-Fe_2O_3), the most stable iron oxide under ambient conditions, is commonly used in catalysts[8], gas-sensing materials[9] and pigments[10]. Magnetite (Fe_3O_4) is by far the most studied phase, and is applied for biomedical applications, being environmental friendly, easy to synthesize and presenting a high saturation magnetization[11]. Iron (Fe) is one of the mostly used metals for industrial applications. To date, various methods have been used for 1D magnetic nanomaterials, such as template assisted electrodeposition[12], nanolithography[13], organometallic chemistry[14], solvothermal[15] and electrospinning technique[16,17]. Among the prior researches on the synthesis of the nanowires, electrospinning technique seems to be the simplest and most versatile technique capable of generating 1D nanowires with diameter on the micro- or nanometers and lengths up to kilometers. Electrospinning is a process by which very fine fibres are drawn from a liquid by an electrical charge, which was first issued by A. Formhals in 1934[18]. Electrospinning combined with heat treatments has been widely adopted to prepare various 1D nanomaterials because of the simple manufacturing method, low cost, and relatively high production rate. The applicability of many types of materials includes metals[19], metal oxides[9,20], and ferrite[21–23] nanofibers. Herein, we have chosen electrospinning method as an effective way to fabricate Fe_3O_4 and Fe nanowires via partial and full reduction of α-Fe_2O_3.

Recently, with the rapid development of wireless communications, local area network and high frequency circuit devices in the gigahertz range, the electromagnetic interference (EMI) problem has become more serious. Many kinds of microwave absorbers have attracted a great deal of interest for solving this problem. As reported in previous literatures, 1D magnetic nanowires showed high anisotropy field, which may result in magnetic resonance shifting to higher frequency, suggesting that it can be used as electromagnetic absorbers in the high

frequency range[24]. Bo Gao and co-workers proposed the Ni nanowires as the absorber filler and the maximum reflection loss of the absorber can reach -8.5 dB at 10 GHz[25]. Ruey-Bin Yang investigated the microwave absorbing properties of iron nanowire at x-band frequencies and the optimal absorption peak reached -10.5 dB ($>90\%$ power absorption) and -15.5 dB ($>97\%$ power absorption), respectively[26]. However, to our best knowledge, the microwave absorption properties of the Fe_3O_4 nanowires have not been reported so far. Therefore, the microwave absorption properties of the as-prepared Fe_3O_4 nanowires/paraffin composite were also discussed in this paper.

Experimental section

Synthesis. In a typical synthesis of Fe_3O_4 and Fe nanowires, we first prepared α-Fe_2O_3 nanowires by the combination of electrospinning and sol-gel process. To electrospin precursor composite wires, Fe nitrate nonahydrate ($Fe(NO_3)_3 \cdot 9H_2O$) was dissolved in a mixed solvent containing ethanol and N,N-Dimetylformamide (DMF, 99.8% purity) with a weight ratio of 1:1, followed by magnetic stirring for 2 h. Then an appropriate amount of polyvinyl pyrrolidone (PVP, $M_w = 1,300,000$) were added into the above solution and further magnetically stirred for 2 h at room temperature to form a homogeneous solution with PVP concentration of 8 wt.%. Subsequently, the prepared sol-gel was transferred into a syringe for electrospining. The electrospinning process was performed by a dedicated electrospinning facility at 14 kV DC voltage, 14 cm spacing between metal needle tip and conductive collector (a piece of flat aluminum foil), and a feed rate was fixed with 0.5 mL/h using a peristaltic pump. During the electrospinning process, the solvent evaporated and a charged fiber was deposited on to the collector. And then the collected fibers were calcined at 550°C for 2 h in air to obtain α-Fe_2O_3 nanowires., Reduction for Fe_3O_4 nanowires was achieved by heating at 250°C for 1 h under a 20 ml/min H_2 and reduction for Fe nanowires was achieved by heating at 350°C for 1 h under a 20 ml/min H_2 atmosphere.

Characterization. The composition and phase purity of the as-synthesized samples were analyzed by X-ray diffraction (XRD, Philips X'Pert PRO) with monochromatized Cu Kα (λ=0.15418 nm) incident radiation. The size distribution and morphologies of the samples were characterized by field-emission scanning electron microscope (FE-SEM,

Hitachi S-4800). The transmission electron microscope (TEM, JEOL JEM-2100) was used for morphology and lattice fringe observation. Magnetization measurements of the typical samples were performed on a vibrating sample magnetometer (VSM, Lakeshore 7304). Magnetic hysteresis loop measurements were performed at 12 kOe at 300 K. The magnetic Fe_3O_4 nanowires/paraffin composite was prepared by uniformly mixing the nanowires in a paraffin matrix and then pressing the mixture into a toroidal shape compact (Φ_{outer}=7.00 mm and Φ_{inner}=3.04 mm). The electromagnetic parameters of the composite with 50 wt% of the microwires were measured in the 0.1–10 GHz range by using an Agilent N5247A vector network analyzer (VNA).

Results and Discussion

The structure and phase composition of the precursor α-Fe_2O_3 and the as-transformed samples were characterized by powder X-ray diffraction (XRD). As shown in Figure 1a, the precursor is pure α-Fe_2O_3 phase (hematite, JCPDS No. 24-0072), which has a rhombohedral structure with the lattice parameters of the a=0.50320 nm and c=1.37619 nm. The XRD patterns of the two as-prepared samples after phase transformation are shown in Figure 1b–1c. The pattern b matches well with the cubic Fe_3O_4 (magnetite, JCPDS No. 65-3107), with lattice parameter of a=0.8393 nm. The sharp reflections of the XRD pattern of iron (figure 1d) can be attributed to the body-centered cubic phase of Fe (JCPDS No. 87-0721), without indication of the precursor or other crystalline byproducts (such as magnetite Fe_3O_4 phase). The XRD patterns reveal that complete phase transformation could be achieved by the method used here.

Conversion of the α-Fe_2O_3 structure to Fe_3O_4 spinel involves a change from a hexagonal close-packed oxide ion array (α-Fe_2O_3) to a cubic close-packed array (Fe_3O_4). This is not a topotactic phase change. The representative overview FE-SEM images of the as-synthesized samples are shown in Figure 2, Figure 3a and Figure 4a. Compared with that of the precursor α-Fe_2O_3, we can see that on conversion from α-Fe_2O_3 to Fe_3O_4 not only the nanowire morphology but also the size is perfectly maintained. As shown in Figure 3b and 3c, the high-magnification images of the nanowires, all wires have similar structure, which is the same as the precursor α-Fe_2O_3 nanowires. The diameter of the nanowires is approximately 50–60 nm. However, by carefully comparing the FE-SEM images, it is

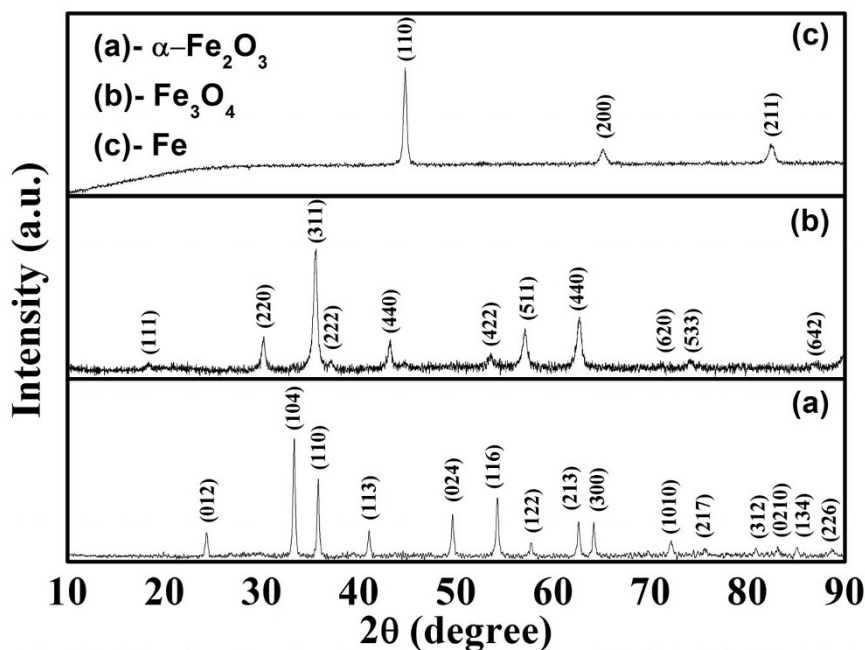**Figure 1 | XRD patterns of the typical as-prepared samples.** (a) α-Fe_2O_3, (b) Fe_3O_4 and (c) Fe nanowires.

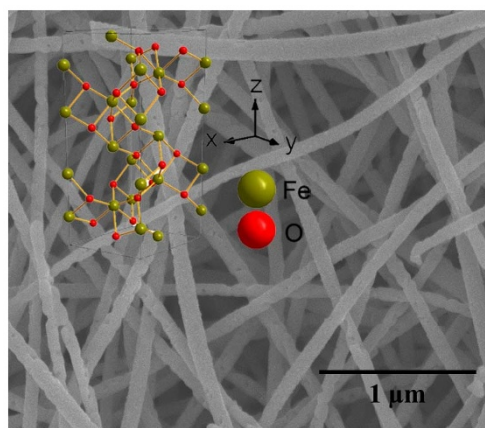**Figure 2 | SEM image of α-Fe₂O₃ nanowire microstructures.** Inset is the crystal structure of α-Fe₂O₃.

found that the surface of the α-Fe$_2$O$_3$ nanowires is smoother than that of Fe$_3$O$_4$ nanowires. To further characterize the structure of Fe$_3$O$_4$ nanowires, Figure 3d shows the lattice-resolution HRTEM image of the nanowires marked by Black Square in Figure 3c, revealing the single-crystalline structure. The interplanar spacing is measured to be 0.253 nm, consistent with the (311) crystallographic orientation of cubic magnetite Fe$_3$O$_4$. In addition, the insets of panel (a) of Figure 2 and panel (a) of Figure 3 are schematic diagrams for the unit cell of α-Fe$_2$O$_3$ and Fe$_3$O$_4$, which clearly verifies that the conversion from α-Fe$_2$O$_3$ to Fe$_3$O$_4$ involves sheaving of the oxide ion planes from AB to ABC stacking, not a topotactic phase change.

When the precursor α-Fe$_2$O$_3$ nanowires were fully reduced under an appropriate temperature, Fe nanowires were still obtained, as shown in Figure 4. The inset of panel (a) of Figure 4 clearly indicates the crystal structure of Fe, which confirms the body-centered cubic phase of the Fe nanowires. From panel (b) and (c) of Figure 4, we found that although the morphology is preserved, there is an evident change in the size. The size of the whole nanowire is reduced on conversion from α-Fe$_2$O$_3$ to Fe (30–40 nm). In addition to this, some of the nanowires have completely broken into two wires. The reason
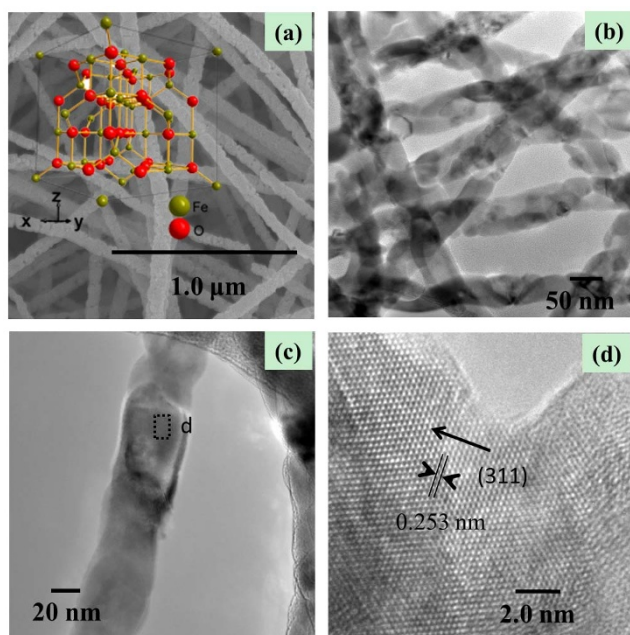

Figure 3 | (a) SEM, (b, c) TEM, (d) HRTEM images of Fe₃O₄ nanowire microstructures. Inset of panel (a) is the crystal structure of Fe₃O₄.
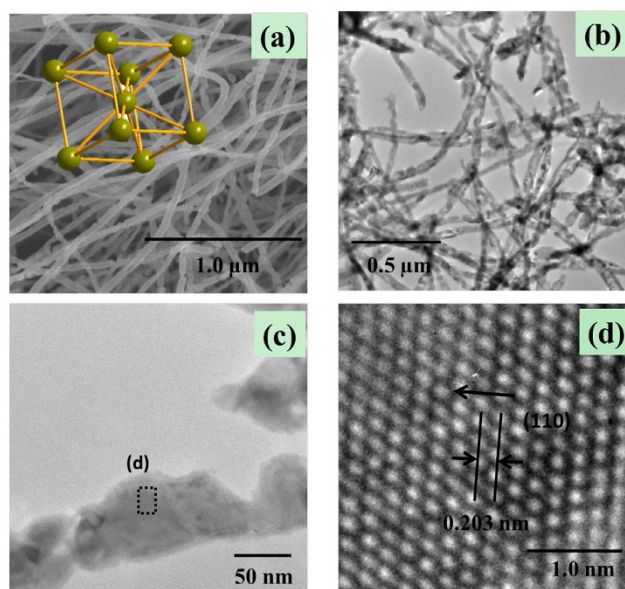

Figure 4 | (a) SEM, (b, c) TEM, (d) HRTEM images of Fe nanowire microstructures. Inset of panel (a) is the crystal structure of Fe.

may be that, for the conversion from α-Fe$_2$O$_3$ to Fe, the final Fe phase must get rid of all oxygen atoms, resulting in a reduced size and shrinkage of the structure. Panel (d) of figure 4 show HRTEM images in the area labeled in panel (c) of Figure 4. It is obvious seen that the image show clear lattice fringes. The lattice spacing of 0.203 nm between adjacent lattice planes is corresponding to the distance between two (110) crystal planes.

We know that iron-based materials often have intriguing magnetic properties because of the structure, while the shape anisotropy and crystallinity can evidently influence the magnetic properties of the microstructured and nanostructured materials. Therefore, we examined the magnetic properties of Fe$_3$O$_4$ and Fe nanowires by VSM at 300 K, shown in figure 5. It can be seen that the saturation magnetization values of Fe$_3$O$_4$ and Fe nanowires are approximately 57.7 emu/g and 133.9 emu/g with the external field of 12 KOe, which are lower than that of corresponding bulk materials ($M_{s(Fe3O4)}$ =96.5 emu/g; $M_{s(Fe)}$ = 217.6 emu/g, 300 K). The lower saturation magnetization is normal for nanomaterials, which is mainly due to the high surface-to-volume ratio for nanomaterials. The spin disorder on the surface and surface oxidation would significantly reduce the total magnetic moments. The inset panel clearly shows the coercivity H_c values are about 479 Oe and 188 Oe for Fe and Fe$_3$O$_4$ nanowires, respectively, which are about 2 orders of magnitude higher than that of bulk materials. The enhancement of coercivity may be due to the shape anisotropy of the nanowire structure.

To reveal the microwave absorption properties of the as-synthesized sample, the frequency dependence of reflection loss (RL) values for Fe$_3$O$_4$ nanowires/paraffin composite backed by a perfect conductive plate was estimated from the complex permeability ($\mu=\mu'-j\mu''$) and permittivity ($\varepsilon=\varepsilon'-j\varepsilon''$) according to the transmit line theory as the following equations[27]:

$$Z_{in} = Z_0 \sqrt{\frac{\mu(f)}{\varepsilon(f)}} \tanh\left[\left(j\frac{2\pi ft}{c}\right)\sqrt{\mu(f)\varepsilon(f)}\right], \qquad (1)$$

$$RL(dB) = 20 \log\left|\frac{Z_{in}/Z_0-1}{Z_{in}/Z_0+1}\right|, \qquad (2)$$

where f is the microwave frequency, t is the thickness of the absorber, c is the velocity of light, Z_0 is the impedance of air and Z_{in} is the input impedance of the absorber.
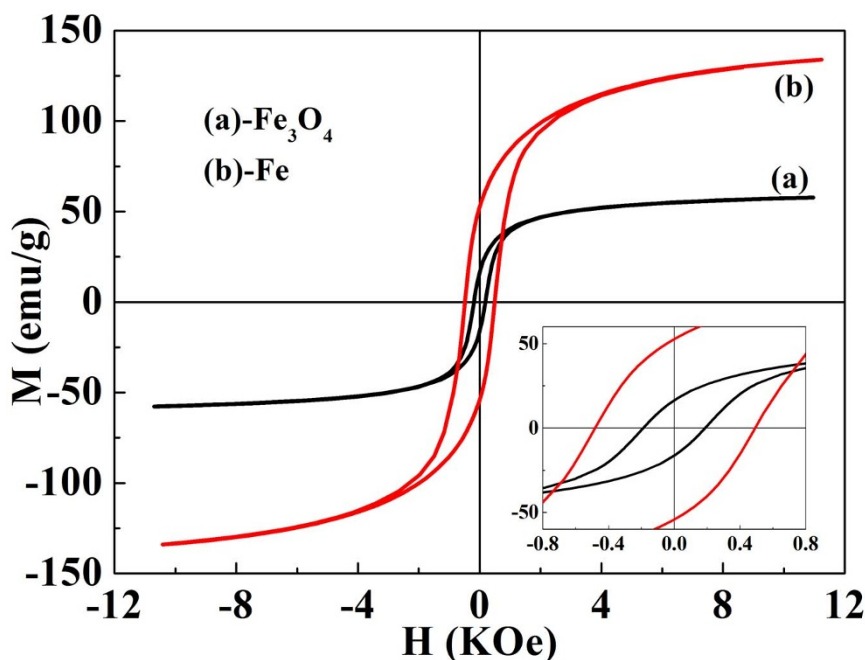
Figure 5 | Magnetic hysteresis loops of (a) Fe$_3$O$_4$ and (b) Fe nanowires. Inset of panel are expanded low field hysteresis curves.

To obtain the microwave absorption properties of Fe$_3$O$_4$ nanowires, we independently measured the complex permittivity and permeability of the sample. Figure 6 shows the complex permittivity and permeability for Fe$_3$O$_4$ nanowires/paraffin composite in the frequency range of 0.1–10 GHz. It is obviously seen that the real part of permittivity ε′ values negligibly decrease with the increasing frequency from 5.7 to 4.5, while the imaginary part ε″ values almost remain constant in the whole frequency range. On the other hand, the permeability spectra exhibit a relaxation type, the real permeability μ′ value obviously decreases from 1.9 to 0.9 with increasing frequency, while the imaginary part of permeability μ″ exhibits a strong peak at 3.3 GHz. The natural resonance frequency (3.3 GHz) is higher than that of the counterpart in nature (1.2 GHz), which may be attributed to the increase of the shape anisotropy. The shape anisotropy fields add to the total anisotropy field and consequently increases the resonance frequency. Here the perturbation with the frequency range of 7–10 GHz is due to the sensitive of the vector network analyzer.

According to equation (1) and (2), the thickness of the absorber is one of the crucial parameters that affect the intensity and the position of the RL peak. Therefore, we simulated the frequency dependence of RL under various matching thicknesses, shown in figure 7(a). The minimum RL for every thickness t$_m$ is obtained (figure 7a black symbol and line). As shown in figure 7a, the Fe$_3$O$_4$ nanowires exhibit excellent microwave absorption properties. A minimum RL reaches −17.2 dB at 6.2 GHz with the thickness of 5.5 mm, which is higher than the aforementioned results of ref. 25, 26. Moreover, at the minimum RL point, the modulus of the ratio between the complex permittivity and permeability |ε/μ| (4.6) is far away from unity, which is quite different from the traditional opinions.

The minimum RL values are obtained at given frequencies if the thickness of the absorber satisfies:

$$t_m = \frac{c}{4f_m(\sqrt{|\mu(f_m)\varepsilon(f_m)|})}, \qquad (3)$$

where c is the velocity of the light in vacuum, $\mu(f_m)$ and $\varepsilon(f_m)$ are the complex permeability and permittivity at f_m, f_m and t_m corresponding to the minimum RL$_{min}$, is defined as the matching frequency and the matching thickness.

Fig. 7(b) shows the dependence of calculated thicknesses (t_{cal}, black line) based on Eq. (3) and the matching thicknesses (t_{mat}, asteroid dots) based on Eq. (1) and Eq. (2) on the matching frequency (f_m). It is obviously that the matching thicknesses are well consistent with the calculated ones, which demonstrates that the frequency of microwave absorption peak obeys the quarter-wavelength model.
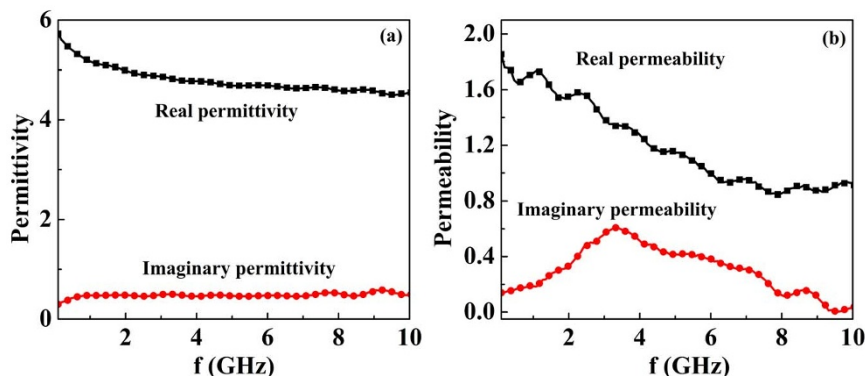

Figure 6 | The complex permittivity (a) and permeability (b) for Fe$_3$O$_4$ nanowires/paraffin composite.
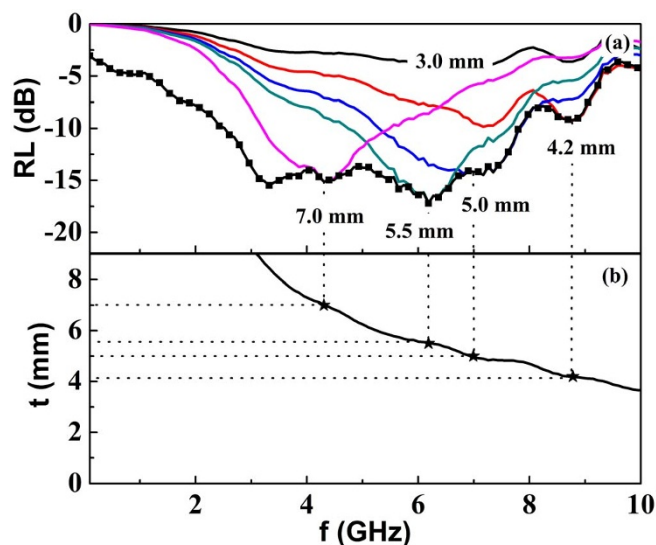
Figure 7 | (a) the frequency dependence of RL (line, Black: 3.0 mm, Red: 4.2 mm, Blue: 5.0 mm, Cyan: 5.5 mm, Magenta: 7.0 mm), the minimum reflection loss for every thickness (symbol and line) and (b) the dependence of matching thickness (t_{mat}) and calculated thickness (t_{cal}) on the matching frequency (f_m). The vertical dot lines are extended from the RL peaks in (a), each line from the RL peak under an absorber thickness crosses with its corresponding thickness contour in (b). The crossover points are indicated by the asteroid dots.

Conclusions

In conclusion, we have successfully synthesized the Fe_3O_4 and Fe nanowires via partial and full reduction of α-Fe_2O_3 obtained by electrospinning method. The microwave absorption properties and the reflection loss mechanism of the prepared Fe_3O_4 nanowires have been investigated carefully. Microwave absorption analysis indicates that the Fe_3O_4 nanowires exhibit excellent microwave absorbability. A minimum RL reaches −17.2 dB at 6.2 GHz. The modulus of the ratio between the complex permittivity and permeability |ε/μ| is far away from unity at the minimum RL point, which is quite different from the traditional opinions. Moreover, the frequency of microwave absorption peak for the Fe_3O_4 nanowires obeys the quarter-wavelength model.

1. Xia, Y. & Yang, P. Guest Editorial: Chemistry and Physics of Nanowires. *Adv. Mater.* **15**, 351–352 (2003).
2. Wu, H., Zhang, R., Liu, X., Lin, D. & Pan, W. Electrospinning of Fe, Co, and Ni Nanofibers: Synthesis, Assembly, and Magnetic Properties. *Chem. Mater.* **19**, 3506–3511 (2007).
3. Eid, C. *et al.* Iron-based 1D nanostructures by electrospinning process. *Nanotechnology* **21**, 125701 (2010).
4. Henry, Y. *et al.* Magnetic anisotropy and domain patterns in electrodeposited cobalt nanowires. *The Euro. Phys. Jour. B* **20**, 35–54 (2001).
5. Sun, G., Dong, B., Cao, M., Wei, B. & Hu, C. Hierarchical Dendrite-Like Magnetic Materials of Fe3O4, γ-Fe2O3, and Fe with High Performance of Microwave Absorption. *Chem. Mater.* **23**, 1587–1593 (2011).
6. Redl, F. X., Cho, K. S., Murray, C. B. & O'Brien, S. Three-dimensional binary superlattices of magnetic nanocrystals and semiconductor quantum dots. *Nature* **423**, 968–971 (2003).
7. Ouyang, M. & Awschalom, D. D. Coherent Spin Transfer Between Molecularly Bridged Quantum Dots. *Science* **301**, 1074–1078 (2003).
8. Brown, A. S. C., Hargreaves, J. S. J. & Rijniersce, B. A study of the structural and catalytic effects of sulfation on iron oxide catalysts prepared from goethite and ferrihydrite precursors for methane oxidation. *Catal. Lett.* **53**, 7–13 (1998).
9. Zheng, W. *et al.* Electrospinning route for α-Fe2O3 ceramic nanofibers and their gas sensing properties. *Mater. Res. Bull.* **44**, 1432–1436 (2009).
10. Zboril, R., Mashlan, M. & Petridis, D. Iron(III) Oxides from Thermal ProcessesSynthesis, Structural and Magnetic Properties, Mössbauer Spectroscopy Characterization and Applications. *Chem. Mater.* **14**, 969–982 (2002).
11. Lin, C. R., Tsai, T. C., Chung, M. & Lu, S. Z. Synthesis and characterization of magnetic nanoparticles embedded in polyvinyl pyrrolidone nanofiber film by electrospinning method. *J. Appl. Phys.* **105**, 07B509 (2009).
12. Nielsch, K., Müller, F., Li, A. P. & Gösele, U. Uniform Nickel Deposition into Ordered Alumina Pores by Pulsed Electrodeposition. *Adv. Mater.* **12**, 582–586 (2000).
13. Serrano-Ramon, L. *et al.* Ultrasmall Functional Ferromagnetic Nanostructures Grown by Focused Electron-Beam-Induced Deposition. *ACS Nano* **5**, 7781–7787 (2011).
14. Dumestre, F. *et al.* Shape control of thermodynamically stable cobalt nanorods through organometallic chemistry. *Angew. Chem. Int. Edit.* **41**, 4286–4289 (2002).
15. Zhang, Z. *et al.* High-Yield Solvothermal Formation of Magnetic CoPt Alloy Nanowires. *J. Am. Chem. Soc.* **125**, 7528–7529 (2003).
16. Barakat, N. A. M. *et al.* CoNi Bimetallic Nanofibers by Electrospinning: Nickel-Based Soft Magnetic Material with Improved Magnetic Properties. *J. Phys. Chem. C* **114**, 15589–15593 (2010).
17. Cavaliere, S. *et al.* Elaboration and characterization of magnetic nanocomposite fibers by electrospinning. *J. Nanopart. Res.* **12**, 2735–2740 (2010).
18. Formhals, A. inventors; Process and apparatus for prepartificial threads. United States patent US 1975504. 1934 Oct 2.
19. Wu, H., Zhang, R., Liu, X., Lin, D. & Pan, W. Electrospinning of Fe, Co, and Ni Nanofibers: Synthesis, Assembly, and Magnetic Properties. *Chem. Mater.* **19**, 3506–3511 (2009).
20. Cheng, Y. *et al.* Formation mechanism of Fe2O3 hollow fibers by direct annealing of the electrospun composite fibers and their magnetic, electrochemical properties. *CrystEngComm* **13**, 2863 (2011).
21. Zhang, J. *et al.* Nanoscale characterization and magnetic reversal mechanism investigation of electrospun NiFe2O4 multi-particle-chain nanofibres. *Nanoscale* **4**, 2754–2759 (2012).
22. Zhang, J. *et al.* BaFe12O19 Single-Particle-Chain Nanofibers: Preparation, Characterization, Formation Principle, and Magnetization Reversal Mechanism. *ACS Nano* **6**, 2273–2280 (2012).
23. Fu, J. *et al.* Unique magnetic properties and magnetization reversal process of CoFe2O4 nanotubes fabricated by electrospinning. *Nanoscale* **4**, 3932 (2012).
24. Liu, J. R., Itoh, M., Terada, M., Horikawa, T. & Machida, K.-i. Enhanced electromagnetic wave absorption properties of Fe nanowires in gigaherz range. *Appl. Phys. Lett.* **91**, 093101 (2007).
25. Gao, B. *et al.* Microwave absorption properties of the Ni nanowires composite. *J. Phys.D: Appl. Phys.* **41**, 235005 (2008).
26. Yang, R. B. *et al.* Microwave absorbing properties of iron nanowire at x-band frequencies. *J. Appl. Phys.* **109**, 07B527 (2011).
27. Liu, J. R., Itoh, M. & Machida, K.-i. Electromagnetic wave absorption properties of alpha-Fe/Fe[sub 3]B/Y[sub 2]O[sub 3] nanocomposites in gigahertz range. *Appl. Phys. Lett.* **83**, 4017–4019 (2003).

Author contributions

R.H.wrote the main manuscript text, W.W.P. prepared the nanowires, W.L., M.G.Z., D.Z. and F.S.L. discussed the microwave properties of the nanowires. All authors reviewed the manuscript.

Additional information

Competing financial interests: The authors declare no competing financial interests.

How to cite this article: Han, R. *et al.* 1D Magnetic Materials of Fe3O4 and Fe with High Performance of Microwave Absorption Fabricated by Electrospinning Method. *Sci. Rep.* **4**, 7493; DOI:10.1038/srep07493 (2014).